Available online at www.sciencedirect.com

SCIENCE DIRECT

Journal of the European Ceramic Society 25 (2005) 599–604

www.elsevier.com/locate/jeurceramsoc

Distribution of fibre pullout length and interface shear strength within a single fibre bundle for an orthogonal 3-D woven Si–Ti–C–O fibre/Si–Ti–C–O matrix composite tested at 1100 °C in air

Ian J. Davies [a,*], Toshio Ogasawara [b], Takashi Ishikawa [b]

[a] *Department of Mechanical Engineering, Curtin University of Technology, G.P.O. Box U1987, Perth, WA 6845, Australia*
[b] *Advanced Composite Evaluation Technology Center, Institute of Space Technology and Aeronautics (ISTA), Japan Aerospace Exploration Agency (JAXA), 6-13-1 Ohsawa, Mitaka-Shi, Tokyo 181-0015, Japan*

Received 16 December 2003; received in revised form 10 March 2004; accepted 21 March 2004

Available online 15 June 2004

Abstract

The distributions of fibre strength, pullout length, and fibre/matrix interface shear strength within a single fibre bundle were investigated for a 3-D woven SiC/SiC composite tensile tested at 1100 °C in air. Fibre pullout lengths were largest at the fibre bundle centre with an embrittled region of approximate width 15 μm at the perimeter. Whereas the fibre strength varied by less than a factor of 2 across the fibre bundle, the fibre/matrix interface shear strength varied by a factor of ~23 with a minimum (100 ± 16 MPa) at the centre and a maximum (2.25 ± 0.21 GPa) close to the embrittled region. The minimum fibre/matrix interface shear strength required for the transition between pseudo-ductile and brittle behaviour was thus estimated to be 2.25 ± 0.21 GPa for this composite system.

Keywords: Composites; Failure analysis; Fibres; Interfaces; SiC/SiC

1. Introduction

The mechanical properties of ceramic matrix composites (CMCs) are known to be greatly influenced by the fibre strength Weibull parameters, S_o and m, measured in situ the composite together with the fibre/matrix interface shear strength, τ.[1] Whilst the largest values of tensile strength, σ, for CMCs have generally been achieved using low values of τ (typically <10 MPa[2]) with subsequently large fibre pullout lengths on the order of several hundred microns,[3] recent work has shown τ values of 370 MPa to also be consistent with superior mechanical properties.[4] An essential aspect of high strength CMCs is their use of fibre/matrix interfaces based on weakly bonded materials such as pyrolytic carbon (py-C),[5] boron nitride (BN),[6] and La-monazite ($LaPO_4$).[7] However, the extreme oxygen sensitivity of py-C and BN above 500 °C is a major cause for concern in CMCs that typically exhibit low-stress matrix microcracking.[8] Oxidation of the fibre/matrix interface[9] and exposed fibre surfaces[10–13] may increase τ to such an extent that crack deflection mechanisms at the fibre/matrix interface are suppressed,[14] leading to the formation of an embrittled region characterised by flat fibre fracture surfaces and negligible pullout lengths.[3,15] A related concern for CMCs containing fibres based on the silicon carbide (SiC) system is the formation of an oxide film at the fibre surface,[15] which acts as a flaw population and decreases fibre strength.[16]

Modelling of the oxidation behaviour in CMCs based on the SiC/SiC system has indicated the maximum oxidation rate to occur at intermediate temperatures (e.g. 500–900 °C[17]) with the rate decreasing at higher temperatures (e.g. ≥1100 °C[18]) due to sealing of cracks at the specimen surface;[18,19] oxidation resistance was also found to increase with use of thin (≤0.1 μm) py-C interfaces.[18]

Although several researchers have experimentally investigated the effects of oxidation on SiC/SiC composites containing py-C[2,20–24] and BN[25–27] interfaces, in addition to other CMCs containing SiC fibres,[28] relatively little data is available for the values of S_o, m, and τ within partially oxidised CMCs, particularly for the variation of these properties within individual fibre bundles. Such information

* Corresponding author.
E-mail address: I.Davies@curtin.edu.au (I.J. Davies).

0955-2219/$ – see front matter © 2004 Elsevier Ltd. All rights reserved.
doi:10.1016/j.jeurceramsoc.2004.03.022

may, for example, shed light on the value of τ required for the suppression of crack deflection mechanisms in SiC/SiC composites. Thus, the present work will concern itself with the investigation of mechanical and physical properties within a single fibre bundle for an orthogonal 3-D woven SiC/SiC composite tensile tested at 1100 °C in air.

2. Experimental procedure

The composite under investigation, based on the SiC/SiC system, contained Tyranno® LoxM Si–Ti–C–O fibres (800 fibres/bundle) surface-modified so as to achieve a 40 nm carbon-rich layer adjacent to the fibre surface.[29] The aim of the surface modification was to promote crack deflection at the carbon-rich layer within the fibre itself, rather than at the fibre surface as is the case for most CMCs. The fibres were woven into an orthogonal 3-D orthogonal configuration with fibre volume fractions of 0.19, 0.19, and 0.02 in the x, y, and z directions, respectively. Matrix densification of the composite was achieved through the repeated polymer impregnation and pyrolysis (PIP) of a precursor similar to polytitanocarbosilane (PTCS). The use of similar precursors for fibre and matrix components was expected to minimise thermal stresses due to any mismatch in the coefficients of thermal expansion. This composite system is referred to as “NUSK-CMC” from the initials of the collaborating partners[†] and has been the subject of recent work by the authors.[29,30]

Following machining to a suitable test geometry,[29] the composite was heated in air to 1100 °C at 0.75 °C s^{-1}, loaded under tension (parallel to the y-axis) to failure, and furnace cooled (initial rate of 3.3 °C s^{-1}); the total time spent at 1100 °C being on the order of 600 s. Further experimental details are available elsewhere.[8,29,31]

In contrast to the complex non-linear stress/strain behaviour noted for similar specimens tested at room temperature (RT) and 1200 °C in vacuum,[8,29,31] the 1100 °C/air specimen’s stress/strain curve was approximately linear to failure with a low tensile strength (∼55 MPa) compared to the RT (381 ± 41 MPa) and 1200 °C/vacuum (405 ± 39 MPa) cases. In fact, the 1100 °C/air specimen tensile strength was comparable with that of the stress required for propagation of matrix cracks within transverse fibre bundles (∼65 MPa),[8] suggesting that the specimen may have failed upon initial matrix microcracking (or shortly thereafter).

Following failure, the specimen fracture surface was investigated using a scanning electron microscope (SEM) (Model JSM-6300F, JEOL, Tokyo, Japan) and the following parameters measured for each fibre visible within a single randomly chosen fibre bundle near the specimen centre: (i) position within the fibre bundle, (ii) fibre pullout length, h, and (iii) whether the fibre exhibited a fracture mirror (Fig. 1(a)) or was flat and featureless (Fig. 1(b)). A total of 698 fibres (out of the 800 nominally expected) were measured with the difference in number being explained by: (i) shielding of fibres by neighbours, and (ii) the presence of holes where fibres had pulled out.

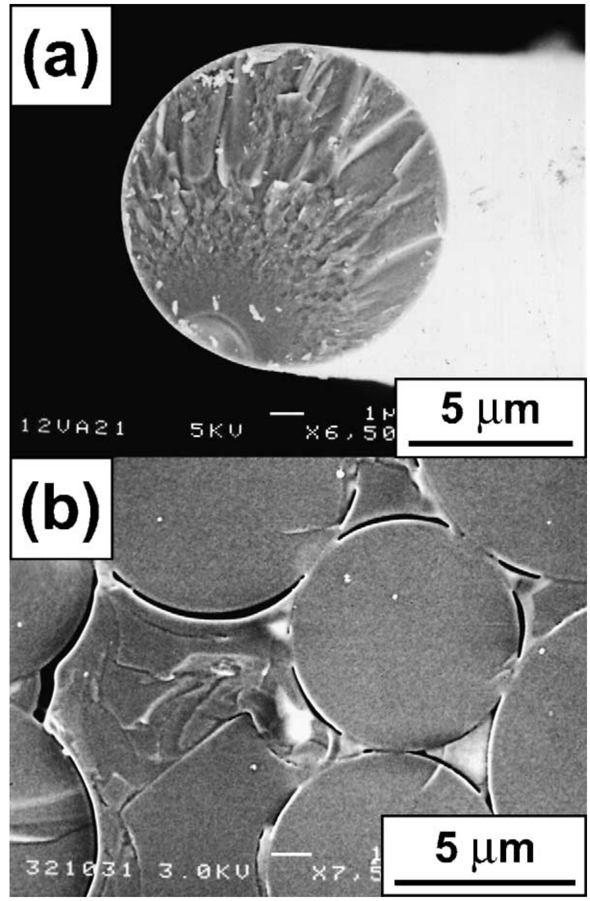

Fig. 1. Scanning electron micrographs illustrating the observed fracture surface types in Tyranno® Si–Ti–C–O fibres: (a) fracture mirror, and (b) flat and featureless.

In addition to the above parameters, due to the likely reaction of oxygen with the fibre surfaces, S_o and m were investigated at the centre and edge of the fibre bundle by measuring the fracture mirror radius, r_m, of individual fibres and using the following relationship to determine the individual fibre strength, S:[32–34]

$$S = \frac{A_m}{\sqrt{r_m}} \quad (1)$$

where A_m is known as the “mirror constant” and was previously determined to be 2.50 ± 0.09 MPa $m^{1/2}$ for the Si–Ti–C–O fibres in situ the composite[35,36] and close to the value of 2.51 MPa $m^{1/2}$ proposed for nominally similar Nicalon® Si–C–O fibres[37] Values of S_o and m were deduced from cumulative failure probability curves of S after applying a suitable correction factor.[38] Fibres within CMCs are known to be effectively tested at a gauge length, δ_c,

† National Aerospace Laboratory of Japan, Ube Industries, Ltd., Shikibo, Ltd., and Kawasaki Heavy Industries, Ltd.

independent of the composite specimen gauge length and to have the form:[1,38]

$$\delta_c = \frac{4\langle h\rangle}{\lambda(m)} = \frac{rS_o}{\tau} \quad (2)$$

where r is the fibre radius (4.03 μm[20]), $\langle h\rangle$ is the mean fibre pullout length, and $\lambda(m)$ is a function only of m. In order to compare values of S_o obtained under different conditions, S_o was normalised to a gauge length, L_o, of 10^{-3} m using the Weibull scaling relationship, i.e.

$$S_o(L_o = 10^{-3} m) = S_o\left(\frac{\delta_c}{10^{-3}}\right)^{1/m} \quad (3)$$

Values of τ within the fibre bundle were estimated using the following rearrangement of Eq. (2):[1,38]

$$\tau = \frac{r\lambda(m)S_o}{4\langle h\rangle} \quad (4)$$

3. Results and discussion

3.1. Fibre pullout length

Fig. 2(a) illustrates the spatial dependence of pullout length within the fibre bundle with it being clear that the majority of fibres, particularly those adjacent to the fibre bundle perimeter, exhibited either zero or negligible fibre pullout and indicative of brittle failure, i.e. suppression of crack deflection mechanisms at the fibre/matrix interface[14] due to τ being excessively high. Further evidence for this

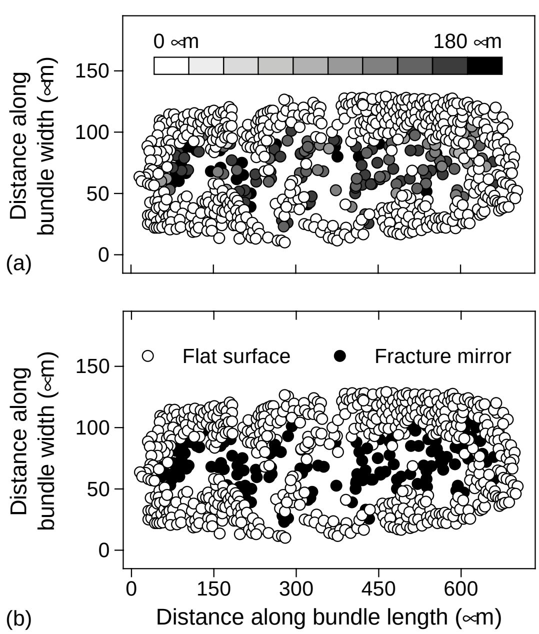

Fig. 2. Positional dependence of properties within a single fibre bundle in an orthogonal 3-D woven SiC/SiC composite tested at 1100 °C in air: (a) fibre pullout length, and (b) existence of flat surface or fracture mirror. Note that fibre pullout lengths in (a) have been shown using a logarithmic scale.

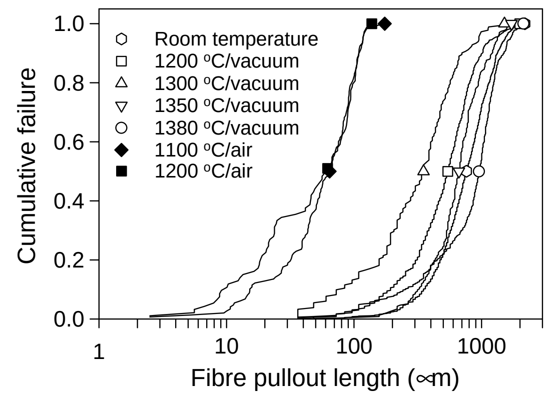

Fig. 3. Fibre pullout length distributions for an orthogonal 3-D woven SiC/SiC composite tested under various conditions 2,20.

has been presented in Fig. 2(b) which indicates a strong correlation between fibres with low h values and the existence of flat fracture surfaces (Fig. 1(b)); in contrast to fracture mirrors (Fig. 1(a)) which typically occur when crack deflection mechanisms are present. That the majority of fibres with significant pullout lengths and fracture mirrors were concentrated towards the centre of the fibre bundle was consistent with previous work[2] that suggested maximum oxidation damage to have occurred at the fibre bundle perimeters. A likely mechanism for this phenomenon would be the propagation of matrix cracks in the transverse fibre bundles,[8] allowing oxygen to access the perimeters of longitudinal (y-axis) fibre bundles.

Although the largest h values were observed at the fibre bundle centre, these values were still considerable smaller when compared to those of specimens tested at RT or in vacuum, i.e. in the absence of oxidation damage. Fig. 3 compares fibre pullout length distributions for specimens tested under a variety of conditions[2,20] with $\langle h\rangle$ for the 1100 °C/air specimen being an order of magnitude lower compared to that of the RT case (810 μm[3]). With reference to Eq. (4), it would thus be expected that τ for the 1100 °C/air specimen, even in the fibre bundle centre where oxidation damage was minimal, would still be significantly larger compared to the values of 5–10 MPa previously measured in non-oxidised specimens.[2]

3.2. Fibre strength parameters

Fibre strength distributions (normalised to a gauge length of 10^{-3} m) at the centre and edge[2] of individual fibre bundles in RT and 1100 °C/air specimens have been presented in Fig. 3 with data for the respective values of S_o and m being given in Table 1. Whereas the centre and edge fibre strength distributions were similar for the RT case (Fig. 4(a)),

[2] For the 1100 °C/air specimen, fibre strengths close to the perimeter could not be measured due to the lack of fracture mirrors (Fig. 2(b)). Data for edge fibres was thus calculated using fibres adjacent to the embrittled region.

Table 1
Values of fibre strength Weibull parameters, S_o and m, measured in situ an orthogonal 3-D woven SiC/SiC composite tested in air

	Room temperature			1100 °C/air		
	S_o (GPa)	S_o (GPa) ($L_o = 10^{-3}$ m)	m	S_o (GPa)	S_o (GPa) ($L_o = 10^{-3}$ m)	m
Centre	3.04 ± 0.02	3.78 ± 0.13	4.18 ± 0.14	4.13 ± 0.03	2.25 ± 0.25	2.96 ± 0.09
Edge	3.15 ± 0.06	3.93 ± 0.13	4.10 ± 0.05	2.45 ± 0.01	1.39 ± 0.15	8.89 ± 0.47

a significant difference was noted for the 1100 °C/air case (Fig. 4(b)) with the normalised S_o for edge fibres being 62% that of the centre value. However, even S_o for the centre fibres (2.25 ± 0.25 GPa) was still considerably below that of the RT specimen (∼3.86 GPa), which itself was approximately 30% below that of the "as received" fibres.[2] The reduction in fibre strength for the 1100 °C/air specimen was attributed to the formation of a surface oxide layer on the fibres;[10–13] the lower strength of the edge fibres being attributed to increased oxidation and hence a thicker oxide layer. Whereas m for fibres in the RT specimen was approximately 4.1, the respective value was 8.89 ± 0.47 for edge fibres in the 1100 °C/air specimen with the increase being attributed to the relatively even thickness of the surface oxide layer. The lower m value for centre fibres in the 1100 °C/air specimen (2.96 ± 0.09) was tentatively attributed to a fraction of the fibres having their strength determined by surface flaws (i.e. similar to the RT case[2]) with the remainder being determined by the surface oxide layer, i.e. two distinct fibre populations. As a first approximation, the authors assumed a linear variation in S_o and m between the centre and furthest fibres with non-zero pullout lengths when applying Eq. (4). This assumption was justified on the ground that, as shown later, changes in τ from Eq. (4) would be dominated by $\langle h \rangle$ rather than S_o or m.

3.3. Mean fibre pullout length

It was next decided to investigate the variation of properties along the fibre bundle minor axis between perimeter and centre with the data in Fig. 2 being divided into (symmetrical) horizontal strips. Whilst this procedure neglects the effects of oxidation from either end of the major axis, the large major/minor axis length ratio would make oxidation along the minor axis by far the dominant component. Results presented in Fig. 5 confirm, as previously mentioned, the existence of a strong correlation between fibres exhibiting pullout and those exhibiting fracture mirror behaviour. In fact, the correlation in Fig. 5 is more specific as it clearly

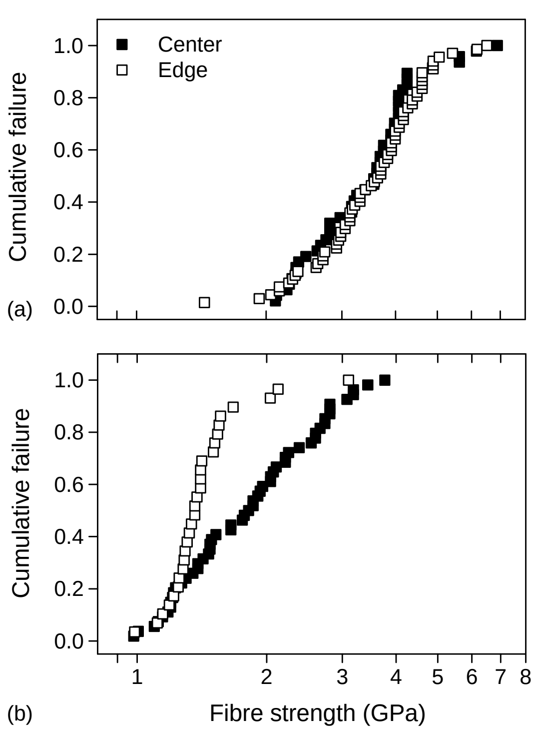

Fig. 4. Fibre strength distributions (normalised to a scale length of 10^{-3} m) measured in situ an orthogonal 3-D woven SiC/SiC composite: (a) room temperature, and (b) 1100 °C in air. "Centre" and "Edge" refer to the general position within the fibre bundle where the measurements were taken.

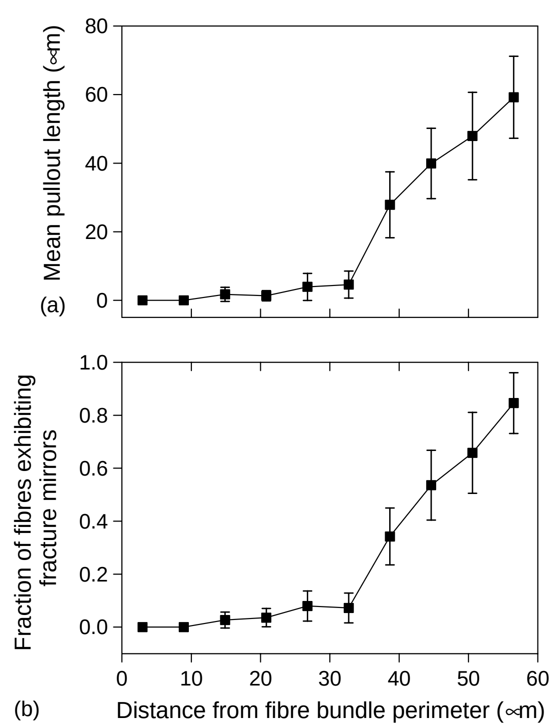

Fig. 5. Distribution of fibre properties along the minor axis within an individual fibre bundle in an orthogonal 3-D woven SiC/SiC composite tested at 1100 °C in air: (a) mean fibre pullout length, $\langle h \rangle$, and (b) fraction of fibres exhibiting fracture mirrors.

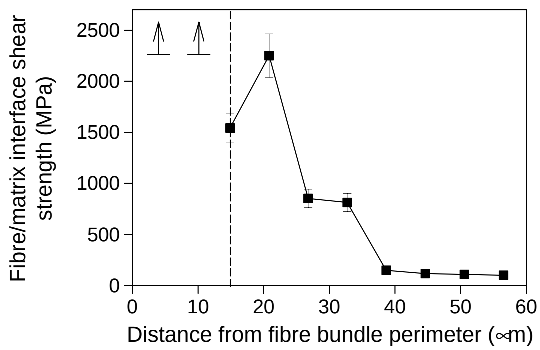

Fig. 6. Distribution of fibre/matrix interface shear strength, τ, along the minor axis within an individual fibre bundle in an orthogonal 3-D woven SiC/SiC composite tested at 1100 °C in air.

indicates the presence of a strong linear relationship between the mean fibre pullout length (Fig. 5(a)) to the fraction, f_m, of fibres exhibiting fracture mirrors (Fig. 5(b)) with $\langle h \rangle = f_m\ (72.3 \pm 1.2)\ \mu m$.

The value of $\langle h \rangle$ varied between zero at the perimeter to 59 µm at the centre with the lowest non-zero value of $\langle h \rangle$ being 1.7 µm at a distance of 15 µm from the bundle perimeter; thus providing an estimate for the width of the embrittled region in this specimen, i.e. 15 µm. It is clear from Eq. (4) that the ratio of $\langle h \rangle$ between fibre bundle centre and lowest non-zero $\langle h \rangle$ region would also provide a first approximation for the ratio of τ between these positions (i.e. 59/1.7) and being even higher for the ratio between centre and perimeter (where $\langle h \rangle$ was zero).

3.4. Fibre/matrix interface shear strength

Values of τ obtained from Eq. (4) have been presented in Fig. 6 with the lowest value of τ being 100 ± 16 MPa at the fibre bundle centre and approximately 20 times that of the RT case,[2] illustrating the rapid increase in τ which results from even a relatively short exposure time to oxygen at elevated temperature. The value of τ gradually increased away from the bundle centre to reach 149 ± 17 MPa at a distance of 39 µm from the bundle perimeter but then increased rapidly to a maximum of 2.25 ± 0.21 GPa adjacent to the embrittled region, with τ being necessarily greater than this within the embrittled region. This value of τ at the transition zone between brittle and non-brittle regions thus provides an estimate of the minimum τ required for suppression of crack deflection mechanisms within this composite system. Whilst such high values of τ have not previously been reported within SiC/SiC composites, the authors attribute this to the lack of quantitative data available in partially oxidised CMCs exhibiting h values on the order of several microns. However, evidence of high strength fibres exhibiting fracture mirrors and micron-range pullout lengths, i.e. the requirements for candidate τ values in the GPa range, is available in the literature,[26,39] suggesting the data presented in this work to not be exceptional for CMCs.

4. Conclusions

The distributions of fibre strength, pullout length, and fibre/matrix interface shear strength, τ, within an individual fibre bundle were investigated for an orthogonal 3-D woven SiC/SiC composite tensile tested at 1100 °C in air. The mean fibre pullout length, $\langle h \rangle$, varied between 59 µm at the centre to zero within an embrittled region (~15 µm width) at the fibre bundle perimeter. Fibre strength (normalised to a gauge length of 10^{-3} m) decreased from 2.25 ± 0.25 GPa at the centre to 1.39 ± 0.15 GPa adjacent to the embrittled region, compared to 3.86 ± 0.13 GPa for a specimen tensile tested at room temperature. The lowest value of τ within the fibre bundle was 100 ± 16 MPa at the centre but this increased rapidly to a maximum of 2.25 ± 0.21 GPa close to the embrittled region, suggesting this value to be a lower bound for τ with respect to suppression of crack deflection mechanisms at the interface in this composite system. Whilst such a wide variation in τ within a single fibre bundle has not previously been noted, this was attributed to the lack of τ data available for composites containing short fibre pullout lengths. Overall, the experimental data was consistent with oxygen having surrounded the fibre bundle perimeter via matrix cracks in the transverse fibre bundles.

Acknowledgements

The authors wish to gratefully acknowledge Dr. M. Shibuya of Ube Industries Ltd., Dr. J. Gotoh of Kawasaki Heavy Industries Ltd., and T. Hirokawa and T. Tanamura of Shikibo Ltd. for the manufacture and supply of all materials used in this study.

References

1. Curtin, W. A., Theory of mechanical properties of ceramic-matrix composites. *J. Am. Ceram. Soc.* 1991, **74**(11), 2837–2845.
2. Davies, I. J., Ishikawa, T., Shibuya, M. and Hirokawa, T., Fibre strength parameters measured in situ for ceramic-matrix composites tested at elevated temperature in vacuum and in air. *Compos. Sci. Technol.* 1999, **59**, 801–811.
3. Davies, I. J., Ishikawa, T., Shibuya, M. and Hirokawa, T., Optical microscopy of a 3-D woven SiC/SiC-based composite. *Compos. Sci. Technol.* 1999, **59**, 429–437.
4. Rebillat, F., Lamon, J., Naslain, R., Lara-Curzio, E., Ferber, M. K. and Besmann, T. M., Interfacial bond strength in SiC/C/SiC composite materials, as studied by single-fibre push-out tests. *J. Am. Ceram. Soc.* 1998, **81**(4), 965–978.
5. Filipuzzi, L., Camus, G., Naslain, R. and Thebault, J., Oxidation mechanisms and kinetics of 1D-SiC/C/SiC composite materials. I. An experimental approach. *J. Am. Ceram. Soc.* 1994, **77**(2), 459–466.
6. Prouhet, S., Camus, G., Labrugere, C., Guette, A. and Martin, E., Mechanical characterization of Si–C(O) fibre/SiC (CVI) matrix composites with a BN-interphase. *J. Am. Ceram. Soc.* 1994, **77**(3), 649–656.
7. Davis, J. B., Hay, R. S., Marshall, D. B., Morgan, P. E. D. and Sayir, A., Influence of interfacial roughness on fibre sliding in oxide composites with La-monazite interphases. *J. Am. Ceram. Soc.* 2003, **86**(2), 305–316.

8. Ogasawara, T., Ishikawa, T., Ito, H., Watanabe, N. and Davies, I. J., Multiple cracking and tensile behavior for an orthogonal 3-D woven Si–Ti–C–O fibre/Si–Ti–C–O matrix composite. *J. Am. Ceram. Soc.* 2001, **84**(7), 1565–1574.
9. Kerans, R. J., Hay, R. S., Parthasarathy, T. A. and Cinibulk, M. K., Interface design for oxidation-resistant ceramic composites. *J. Am. Ceram. Soc.* 2002, **85**(11), 2599–2632.
10. Kakimoto, K., Shimoo, T. and Okamura, K., Oxidation-induced microstructural change of Si–Ti–C–O fibres. *J. Am. Ceram. Soc.* 1998, **81**(2), 409–412.
11. Takeda, M., Urano, A., Sakamoto, J. and Imai, Y., Microstructure and oxidation behavior of silicon carbide fibres derived from polycarbosilane. *J. Am. Ceram. Soc.* 2000, **83**(5), 1171–1176.
12. Shimoo, T., Toyoda, F. and Okamura, K., Thermal stability of low-oxygen silicon carbide fibre Hi-Nicalon subjected to selected oxidation treatment. *J. Am. Ceram. Soc.* 2000, **83**(6), 1450–1456.
13. Shimoo, T., Morita, T. and Okamura, K., Oxidation of low-oxygen silicon carbide fibres (Hi-Nicalon) in carbon dioxide. *J. Am. Ceram. Soc.* 2001, **84**(12), 2975–2980.
14. He, H. and Hutchinson, J. W., Crack deflection at an interface between dissimilar elastic materials. *Int. J. Solid Struct.* 1989, **25**(9), 1053–1067.
15. Woodford, D. A., Van Steele, D. R., Brehm, J. A., Timms, L. A. and Palko, J. E, Testing the tensile properties of ceramic-matrix composites. *JOM* 1993 (May), 57–63.
16. Gogotsi, Y. G. and Yoshimura, M., Low-temperature oxidation, hydrothermal corrosion, and their effects on properties of SiC (Tyranno) fibres. *J. Am. Ceram. Soc.* 1995, **78**(6), 1439–1450.
17. Evans, A. G., Zok, F. W., McMeeking, R. M. and Du, Z. Z., Models of high-temperature, environmentally assisted embrittlement in ceramic-matrix composites. *J. Am. Ceram. Soc.* 1996, **79**(9), 2345–2352.
18. Philipuzzi, L. and Naslain, R., Oxidation mechanisms and kinetics of 1D-SiC/C/SiC composite materials. II. Modeling. *J. Am. Ceram. Soc.* 1994, **77**(2), 467–480.
19. Lamouroux, F., Naslain, R. and Jouin, J.-M., Kinetics and mechanisms of oxidation of 2D woven C/SiC composites. II. Theoretical approach. *J. Am. Ceram. Soc.* 1994, **77**(8), 2058–2068.
20. Davies, I. J., Ishikawa, T., Shibuya, M., Hirokawa, T. and Gotoh, J., Fibre and interfacial properties measured in situ for a 3D woven SiC/SiC-based composite with glass sealant. *Composites: Part A* 1999, **30**, 587–591.
21. Windisch, C. F., Henager, C. H., Springer, G. D. and Jones, R. H., Oxidation of the carbon interface in Nicalon-fibre-reinforced silicon carbide composite. *J. Am. Ceram. Soc.* 1997, **80**(3), 569–574.
22. Lara-Curzio, E., Analysis of oxidation-assisted stress-rupture of continuous fibre-reinforced ceramic matrix composites at intermediate temperatures. *Composites: Part A* 1999, **30**, 549–554.
23. Jones, R. H., Henager, C. H., Lewinsohn, C. A. and Windisch, C. F., Stress-corrosion cracking of silicon carbide fibre/silicon carbide composites. *J. Am. Ceram. Soc.* 2000, **83**(8), 1999–2005.
24. Badini, C., Fino, P., Ubertalli, G. and Taricco, F., Degradation at 1200 °C of a SiC coated 2D-Nicalon/C/SiC composite processed by SICFILL® method. *J. Eur. Ceram. Soc.* 2000, **20**, 1505–1514.
25. More, K. L., Ailey, K. S., Lowden, R. A. and Lin, H. T., Evaluating the effect of oxygen content in BN interfacial coatings on the stability of SiC/BN/SiC composites. *Composites: Part A* 1999, **30**, 463–470.
26. Morscher, G. M., Hurst, J. and Brewer, D., Intermediate-temperature stress rupture of a woven Hi-Nicalon, BN-interphase, SiC-matrix composite in air. *J. Am. Ceram. Soc.* 2000, **83**(6), 1441–1449.
27. Ogbuji, L. U. J. T., Pest-resistance in SiC/BN/SiC composites. *J. Eur. Ceram. Soc.* 2003, **23**, 613–617.
28. Celemin, J. A. and Llorca, J., The embrittlement of Nicalon/alumina composites at intermediate and elevated temperatures. *Compos. Sci. Technol.* 2000, **60**, 1067–1076.
29. Ishikawa, T., Bansaku, K., Watanabe, N., Nomura, Y., Shibuya, M. and Hirokawa, T., Experimental stress/strain behavior of SiC-matrix composites reinforced with Si–Ti–C–O fibres and estimation of matrix elastic modulus. *Compos. Sci. Technol.* 1998, **58**(1), 51–63.
30. Ogasawara, T., Ishikawa, T., Suzuki, N., Davies, I. J., Suzuki, M., Gotoh, J. and Hirokawa, T., Tensile creep behavior of 3-D woven Si–Ti–C–O fibre/SiC-based matrix composite with glass sealant. *J. Mater. Sci.* 2000, **35**, 785–793.
31. Ishikawa, T., Yamamura, T., Hirokawa, T., Hayashi, Y., Noguchi, Y and Matsushima, M., Strength and fracture toughness properties of oxidation resistant high-temperature ceramic matrix composites. In *Proceedings of the Ninth International Conference on Composite Materials (ICCM-9), Vol 2*, ed. A. Miravette. Madrid, Spain, July 1993. Woodhead Publishing Co., Cambridge, UK, 1993, pp. 137–144.
32. Shand, E. B., Breaking stresses of glass determined from dimensions of fracture mirrors. *J. Am. Ceram. Soc.* 1959, **42**(10), 474–477.
33. Levengood, W. C., Effects of original flaw characteristics on glass strength. *J. Appl. Phys.* 1958, **29**(5), 820–826.
34. Krohn, D. A. and Hasselman, D. P. H., Relation of flaw size to mirror in the fracture of glass. *J. Am. Ceram. Soc.* 1971, **54**(8), 411.
35. Davies, I. J. and Ishikawa, T., Estimation of the fracture toughness of Tyranno® Si–Ti–C–O fibres from flaw size and ‘fracture mirror’ data measured in situ a 3-D woven SiC/SiC composite. *Int. J. Mater. Prod. Technol.* 2001, **16**(1–3), 189–196.
36. Davies, I. J. and Ishikawa, T., Estimation of the ‘mirror constant’ for Tyranno® Si–Ti–C–O fibres in situ a 3-D woven SiC/SiC composite. *J. Am. Ceram. Soc.* 2002, **85**(3), 691–693.
37. Eckel, A. J. and Bradt, R. C., Strength distribution of reinforcing fibres in a Nicalon fibre/chemically vapor infiltrated silicon carbide matrix composite. *J. Am. Ceram. Soc.* 1989, **72**(3), 455–458.
38. Curtin, W. A., In situ fibre strengths in ceramic-matrix composites from fracture mirrors. *J. Am. Ceram. Soc.* 1994, **77**(4), 1075–1078.
39. Parthasarathy, T. A., Boakye, E. E., Keller, K. A. and Hay, R. S., Evaluation of porous ZrO_2–SiO_2 and monazite coatings using Nextel™ 720-fibre-reinforced Blackglas™ minicomposites. *J. Am. Ceram. Soc.* 2001, **84**(7), 1526–1532.